

# Deciphering Teneurin Domains That Facilitate Cellular Recognition, Cell–Cell Adhesion, and Neurite Outgrowth Using Atomic Force Microscopy-Based Single-Cell Force Spectroscopy

Jan Beckmann,<sup>†,‡,||</sup> Rajib Schubert,<sup>§,||</sup> Ruth Chiquet-Ehrismann,<sup>\*,†,‡</sup> and Daniel J Müller<sup>\*,§</sup>

<sup>†</sup>Novartis Research Foundation, Friedrich Miescher Institute for Biomedical Research, Maulbeerstrasse 66, 4058 Basel, Switzerland

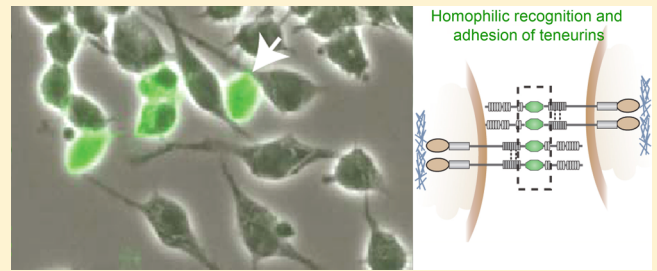
<sup>‡</sup>Faculty of Science, University of Basel, Klingelbergstrasse 50, 4056 Basel, Switzerland

<sup>§</sup>Department of Biosystems Science and Engineering, ETH Zurich, Mattenstrasse 26, 4058 Basel, Switzerland

## Supporting Information

**ABSTRACT:** Teneurins are evolutionarily conserved transmembrane receptors that function as axon guidance and target selection molecules in the developing nervous system. How teneurins recognize each other, whether they establish neuronal adhesion, and which teneurin specific interactions guide neurons remains to be determined. To reveal insight into these pertinent questions we combine atomic force microscopy-based single-cell force spectroscopy with genetic engineering and quantify the interactions teneurins establish between animal cells. Using a combinatorial approach of deletions and swaps of teneurin-1 and teneurin-2 domains, we unravel that teneurins use their NHL (NCL-1, HT2A, and Lin-41) domain to select homophilic teneurins from adjacent cells. This homophilic recognition of teneurins initiates cell–cell adhesion that, dependent on the intracellular domain, strengthens over time. Neurite outgrowth assays show that establishing and strengthening of teneurin-mediated homophilic cell–cell adhesion is required to stop outgrowth. On the basis of the results, we introduce a molecular model of teneurin domains that specify cellular recognition, adhesion strengthening, and neuronal pathfinding. The combined force spectroscopy and genetic approach can be applied to quantitatively decipher the contribution of any neuronal receptor domain and more generally of a given cell surface receptor domain to cell–cell recognition and adhesion.

**KEYWORDS:** *Atomic force microscopy, actomyosin cortex, human embryonic kidney 293 cells, neuronal receptor, neuronal recognition, neuroblastoma*



The assembly of a functional nervous system depends on precisely regulated neurite outgrowth, axon guidance and recognition of the target area to form appropriate synapses. Many molecular cues are known that guide axons and help in neuronal partner matching.<sup>1</sup> Teneurins are a family of evolutionarily conserved cellular receptor proteins<sup>2</sup> that are involved in setting up neuronal circuits in *Drosophila*,<sup>3,4</sup> in mouse,<sup>5</sup> as well as in humans.<sup>6</sup> Teneurins consist of an N-terminal intracellular domain followed by a single span transmembrane domain, and a large extracellular part harboring the following assemblies of repeats: the epidermal growth factor (EGF) domain consisting of eight EGF-like repeats, the NHL domain consisting of several NHL (from NCL-1, HT2A, and Lin-41) repeats, and a YD (tyrosine and aspartate) domain consisting of twenty-six YD repeats (Figure 1A).<sup>2</sup> In vertebrates, four paralogs called teneurin-1 to -4 exist with distinct nonoverlapping patterns of expression in specific subpopulations of neurons.<sup>7,8</sup> Biochemical as well as cell culture experiments suggested that teneurins undergo homophilic (same teneurins) interactions.<sup>9,10</sup> However, it is unknown by which mechanisms teneurins of two neuronal cells recognize each other, whether or not these interactions result in the

formation of adhesive contacts, and how teneurins select and interact with each other to guide neurons.

So far atomic force microscopy (AFM)-based single-cell force spectroscopy (SCFS) has been applied to quantify the adhesive interactions of living cells to molecular resolution.<sup>11,12</sup> This allowed quantifying the contribution of cell surface receptors toward establishing cell–cell adhesion.<sup>11,13</sup> In the present study, we go one important step further and combine SCFS with genetic engineering to characterize the contribution of individual domains of neuronal surface receptors to neuronal outgrowth. Our results unravel that teneurins select for homophilic interaction partners (same teneurins) and function as cell–cell adhesion receptors. Using a combination of deletions and swaps of teneurin-1 and teneurin-2 domains, we identify which teneurin domains facilitate molecular recognition between cells, strengthen cell–cell adhesion, and direct neurite outgrowth. On the basis of these results we introduce a model of how teneurins of neuronal cells interact.

**Received:** April 14, 2013

**Revised:** May 15, 2013

**Published:** May 20, 2013



**Results. Extracellular Domains of Teneurins Establish and Strengthen Homophilic Cell–Cell Adhesion.** To test if teneurins can act as cell–cell adhesion receptors we established an ex vivo system in which human embryonic kidney 293 (HEK293) cells overexpressed either GFP- or RFP-tagged full-length teneurin-1 or -2 from chicken, respectively (Figure 1A). Surface expression was confirmed with antibody staining against the extracellular EGF domains of teneurin-1 or -2 in comparison to the fluorescent protein tag fused to the intracellular N-termini of the teneurins (Figure 1B and Supporting Information Figure S1). The overexpression level of chicken teneurins, which was 20–40-fold higher compared to that of endogenous teneurins expressed by HEK293 cells, was controlled qualitatively and quantitatively using fluorescence microscopy, measuring the mRNA level (Figure 1C), and by FACS sorting (Supporting Information Figure S1A,B). Next, we applied SCFS to quantify the adhesion between HEK293 cells overexpressing teneurins (Figure 1D). SCFS has been established in the past decade to quantify the adhesion strength of live cells from the cellular to molecular scale.<sup>11,12</sup> In our SCFS experiments, we brought two HEK293 cells into contact for a predefined time (ranging from 1 to 120 s) and force (1 nN) allowing the cells to form adhesive contacts. After this initial contact time, both cells were separated and their maximal adhesion force measured (Figure 1D).

In our first set of SCFS experiments, we characterized the adhesive strengths between homotypic and heterotypic couples of HEK293 cells overexpressing either full-length teneurin-1, full-length teneurin-2, and as control HEK293 cells expressing teneurin-2 lacking the extracellular domains (Figure 1E). For all contact times tested, the adhesive force established between cells expressing teneurin-1 or between cells overexpressing teneurin-2 was much higher compared to the adhesive force established between HEK293 cells expressing different teneurins or teneurins devoid of their extracellular domains (Figure 1E,F). This enhanced adhesion was also not observed for wild-type HEK293 cells that did not overexpress teneurin (Supporting Information Figure S1C,D). Furthermore, the adhesive force of cells overexpressing the same full-length teneurins increased strongly with contact time (Figure 1E). Thus, the adhesive contacts formed between teneurin overexpressing cells strengthened over time. The recorded differences in cell–cell adhesion are unlikely to be a consequence of dissimilar morphological or mechanical cell-properties, as neither cell size nor “contact stiffness”<sup>13</sup> correlated with the maximum adhesion forces (Figure 1G). Taken together these results confirm that the strong homophilic adhesion established between teneurin overexpressing cells requires the presence of the teneurin extracellular domains. Furthermore, to establish strong cell–cell adhesion both cells have to express the same type of teneurins including their extracellular domains. In addition, the results demonstrate that teneurins mediate homophilic cell–cell adhesion, which significantly strengthens over time.

**NHL Teneurin Domain Facilitates Homophilic Recognition.** To characterize which of the extracellular teneurin domains facilitate homophilic recognition between cells we took two approaches. In one approach, we deleted one teneurin domain after the other starting at the C-terminus. In the other approach, we swapped domains between teneurin-1 and -2 (Figure 1A). The adhesion between HEK293 cells overexpressing these different teneurin constructs was characterized by SCFS (Figure 2 and Supporting Information Figures S2 and

S3). Cell couples overexpressing teneurin-2 lacking the YD domain could establish the typical strong homophilic adhesion similar to full-length teneurin overexpressing cells (Figure 2A(i)). However, after further deletion of the NHL domain, the cells lost the ability to establish strong adhesion (Figure 2A(ii)). The results did not significantly change when one adhering HEK293 cell overexpressed full-length teneurin-2 and the other cell overexpressed one of the truncated teneurin-2 constructs described (Supporting Information Figure S2A,B). Repeating the same SCFS experiments for HEK293 cells overexpressing teneurin-1 constructs revealed similar results (Supporting Information Figure S2E,F and S3A). These experiments suggest that as soon as one cell lacked the NHL teneurin domain, the cell–cell couple could not establish strong homophilic adhesion.

To investigate whether the NHL repeats alone selected for homophilic cell adhesion, we replaced the NHL domain of teneurin-1 (NHL1) by that of teneurin-2 (NHL2) and vice versa (Figure 1A). Now cells overexpressing teneurin-1 that carried the NHL2 domain could not establish strong homophilic adhesion to cells overexpressing wild-type teneurin-1 but instead these cells established strong “homophilic” adhesion to cells overexpressing teneurin-1 carrying the NHL2 domain and to cells overexpressing teneurin-2 (Figure 2B and Supporting Information Figure S3D). Conversely, strong homophilic adhesion was obtained between cells that overexpressed teneurin-2 carrying the NHL1 domain and any other cells carrying the NHL1 domain but not with cells overexpressing teneurin-2 (Figure 2B and Supporting Information Figure S3C,E). To further characterize the contribution of the EGF domain to the homophilic cell–cell adhesion, we swapped the EGF domains of teneurin-1 and teneurin-2 (Figure 1A). Cells overexpressing these teneurin constructs showed that the NHL domain dependent strong homophilic adhesion is independent of the origin of the EGF domain (Figure 2B and Supporting Information Figure S3F,G). These results clearly demonstrate that the NHL domain of teneurin selects for homophilic interactions between cells.

As final proof for the interaction between NHL domains we tested whether addition of purified NHL domains (Supporting Information Figure S1F) was able to block teneurin-mediated cell–cell adhesion. Therefore, HEK293 cells overexpressing full-length teneurin-1 were allowed to form adhesions in the absence or presence of increasing concentrations of soluble NHL1 domains (Figure 2C). As the NHL1 domain concentration approached 1 μM, homophilic cell–cell adhesion decreased until it was suppressed completely in the presence of 1 mM NHL1 domains. This effect was specific to teneurin-1 mediated cell–cell adhesion since addition of NHL1 domains to HEK293 cells overexpressing teneurin-2 had no effect on their adhesion strength (Figure 2C). In summary, this set of experiments shows that teneurins overexpressed in HEK293 cells establish homophilic recognition as long as they carry the same NHL domains. EGF and YD domains do not contribute to homophilic recognition.

**Intracellular Teneurin Domain Is Essential to Strengthen Cell–Cell Adhesion but Not for Homophilic Recognition.** Next, we investigated the contribution of the intracellular teneurin domain to teneurin-mediated homophilic cell–cell adhesion. We engineered HEK293 cells overexpressing teneurin-2 that lacked the intracellular domain and found that these cells were unable to establish significantly increased adhesion strengths (Figure 2A(iii)). Thus, strengthening of

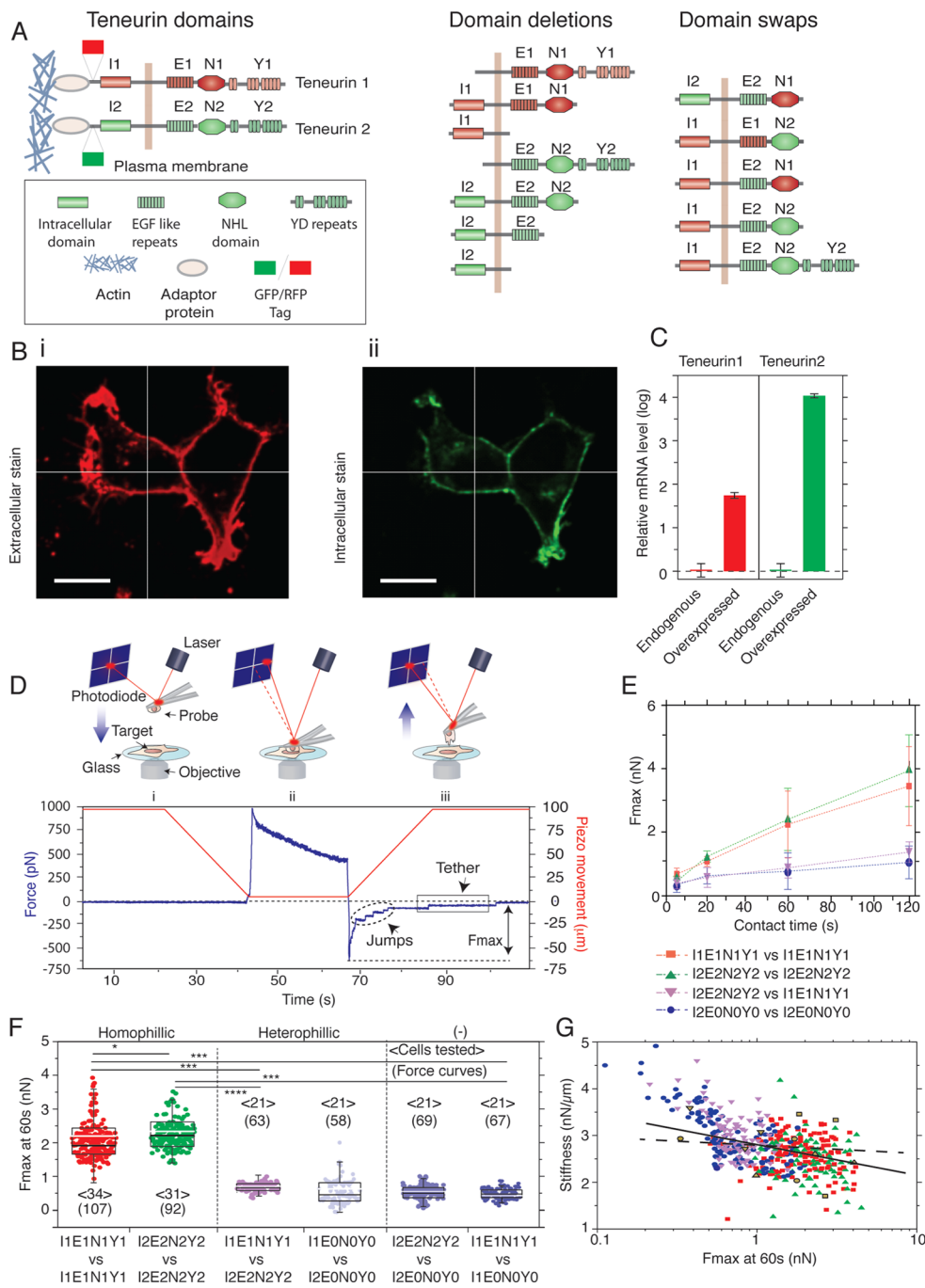


**Figure 1.** Teneurin-mediated cell–cell adhesion assay. (A) Domains, and deletion and swap constructs of teneurin-1 (red) and teneurin-2 (green). Each domain is denoted with a one letter code (I, intracellular; E, EGF; N, NHL; Y, YD) followed by the teneurin number. Possible interactions of the intracellular domain with the actin cytoskeleton are indicated through adaptor proteins, which candidates are CAP/ponsin, vinculin or unknown. (B) Confocal microscopy images of HEK293 cells overexpressing teneurin. (i) Nonpermeabilized cells have been fluorescently stained with antibodies against the EGF domains. (ii) GFP fused to the teneurin intracellular domain is colocalized at the cell membranes. GFP served as reporter for teneurin expression of each HEK293 cell strain (Supporting Information Figure S1). (C) Transcript levels of endogenous and overexpressed teneurin in HEK293 cells. (D) Outline of SCFS experiments. A single (“probe”) cell immobilized on an AFM cantilever is approached into contact with a second “target” cell. After a predefined contact time, the probe cell was retracted at 5  $\mu\text{m}/\text{s}$  and adhesive forces were detected recording the cantilever deflection over the distance traveled by the cantilever. The F–D curve records the maximum adhesion force ( $F_{\text{max}}$ ) between probe and target cell. (E)  $F_{\text{max}}$  as a function of contact time for homophilic and heterophilic adhesion between HEK293 cells overexpressing full-length teneurin-1 (I1E1N1Y1), full-length teneurin-2 (I2E2N2Y2), or extracellular truncated teneurin (I2E0N0Y0). Deleted domains are indicated by their letter code followed by 0. Values are presented as mean and standard errors (SEM) from 14 to 210 (depending on contact time) F–D curves recorded for each contact time. (F) Homophilic versus heterophilic adhesion at 60 s contact time. Data is presented as a box-whisker plot with each data point representing one cell–cell adhesion experiment. Median is white and mean is black.  $P$  values are \*  $p < 0.01$  and \*\*  $p < 0.001$ . (G) Slope (solid line) of contact region (“contact stiffness”) of different cell line combinations (as in E) extracted from the approach F–D curve versus  $F_{\text{max}}$  detected from the retraction F–D curve at 60 s contact time. No statistical correlation ( $r = -0.113$ ) was seen between the different cell lines randomly chosen.

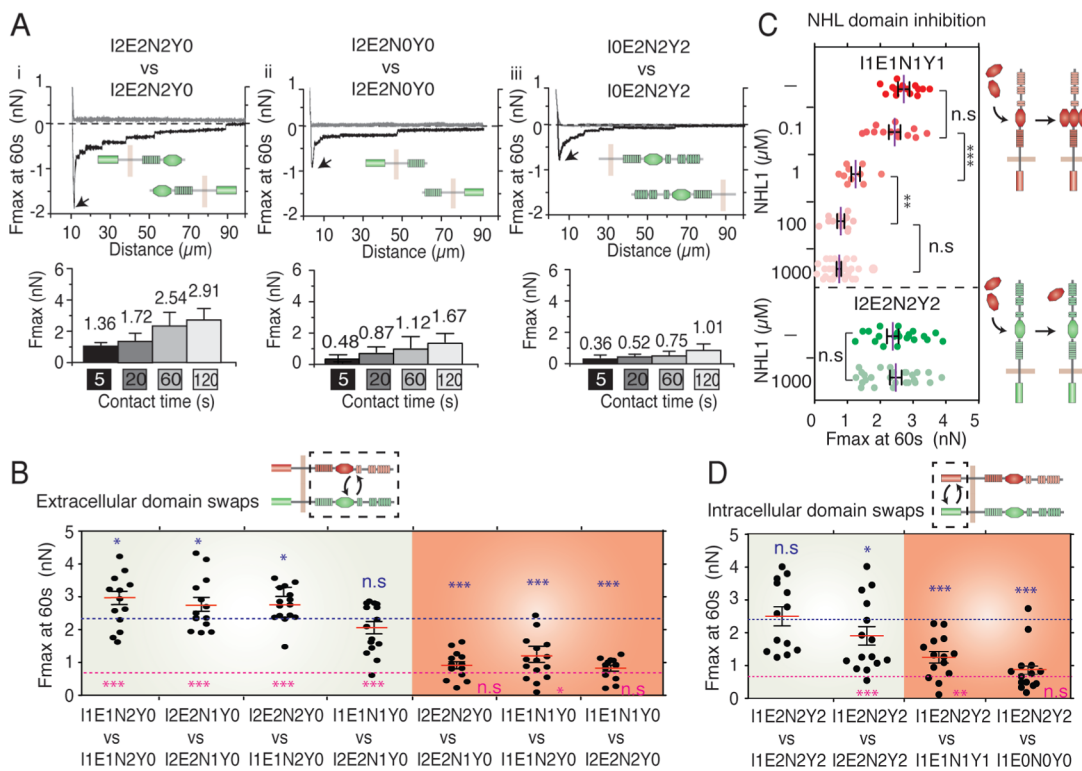


**Figure 2.** Quantification of adhesion forces between HEK293 cells overexpressing different teneurin constructs. (A) Representative F–D curves (60 s contact time) recording the adhesion between HEK293 cells overexpressing different teneurin constructs. F–D curves showing the probe cell approaching the target cell are gray. F–D curves recorded when separating both cells (black) are used to estimate the maximum adhesion force (arrow, Fmax). Histograms show maximal adhesion forces between probe cell and target cell after contact times of 5, 20, 60, and 120 s. Fifteen to 218 (depending on contact time) F–D curves were recorded per condition. Numbers above bars represent mean Fmax values and errors indicate SEM. (B) Maximal adhesion forces between two HEK293 cells overexpressing teneurin constructs having their YD deleted and NHL domains swapped (Figure 1A). Each data point represents Fmax determined for one cell–cell couple, mean adhesion forces are represented as red bars and SEM as black bars. Green-and red-shaded areas highlight high and low cell–cell adhesion forces, respectively. (C) NHL domain inhibition experiments. Maximal adhesion force of homophilic cell–cell couples overexpressing either full-length teneurin-1 (I1E1N1Y1) or teneurin-2 (I2E2N2Y2). Addition of purified teneurin-1 NHL (NHL1) domains inhibits homophilic adhesion mediated by teneurin-1, whereas teneurin-2 mediated adhesion remains unaffected. (D) Maximal adhesion forces between cells overexpressing teneurin constructs with swapped intracellular domains (Figure 1A). P values are \* p < 0.01 and \*\* p < 0.001.

homophilic cell–cell adhesion requires the presence of the intracellular teneurin domain. To answer the question whether the intracellular domain affects homophilic recognition between teneurin expressing cells we swapped the intracellular domains of teneurin-1 and -2 (Figure 1A). Cells overexpressing teneurin-2 constructs carrying the teneurin-1 intracellular domain adhered with similar strength to each other as to wild-type teneurin-2 expressing cells but could not increase adhesion strength to cells overexpressing wild-type teneurin-1 (Figure 2D). All cells exhibiting teneurin versions with identical NHL domains and either the teneurin-1 or the teneurin-2 intracellular domain adhered strongly to each other (Figure 2D, and Supporting Information Figure S3E,H,I). These results show that the intracellular teneurin domain does not affect the selection of the homophilic cell adhesion partner but is required for the strengthening of adhesion.

Intracellular teneurin domains have been implicated in interactions with the cytoskeleton.<sup>4,14</sup> We therefore considered whether or not cytoskeletal interactions are required for teneurins to establish strong cell adhesion. To test whether the actin cytoskeleton is required for strengthening the teneurin-mediated cell–cell adhesion, we perturbed the actomyosin cortex using latrunculin A, which sequesters actin monomers and disrupts actin filaments of the cytoskeleton.<sup>15</sup> In

the presence of 100 nM latrunculin A, teneurin-mediated homophilic cell–cell adhesion showed significantly reduced strength, whereas at 1 μM latrunculin A the strong homophilic cell–cell adhesion disappeared (Figure 3A). However, latrunculin A also reduced the weak adhesion between HEK293 cells that overexpressed teneurin-2 lacking the intracellular domains (Figure 3B). This latter effect is expected because unspecific as well as specific cell adhesion depends on an intact actomyosin cortex. In a next set of experiments, we investigated whether actomyosin contraction was involved in establishing homophilic cell–cell adhesion and used blebbistatin to inhibit myosin II.<sup>16</sup> In the presence of 50 μM blebbistatin, the strong homophilic cell–cell adhesion between teneurin-2 overexpressing cells dropped to the low level of unspecific cell–cell adhesion (Figure 3C). However, upon photoinactivation of blebbistatin<sup>17</sup> the strong homophilic teneurin-2 mediated cell–cell adhesion fully recovered (Figure 3C). In contrast, the weak adhesion between HEK293 cells overexpressing teneurin-2 lacking their intracellular domains was not perturbed by blebbistatin (Figure 3D). In summary, these experiments using latrunculin A and blebbistatin suggest that teneurins anchor via the intracellular domain to the actomyosin cytoskeleton and that this anchorage is required to strengthen teneurin-mediated homophilic cell–cell adhesion.

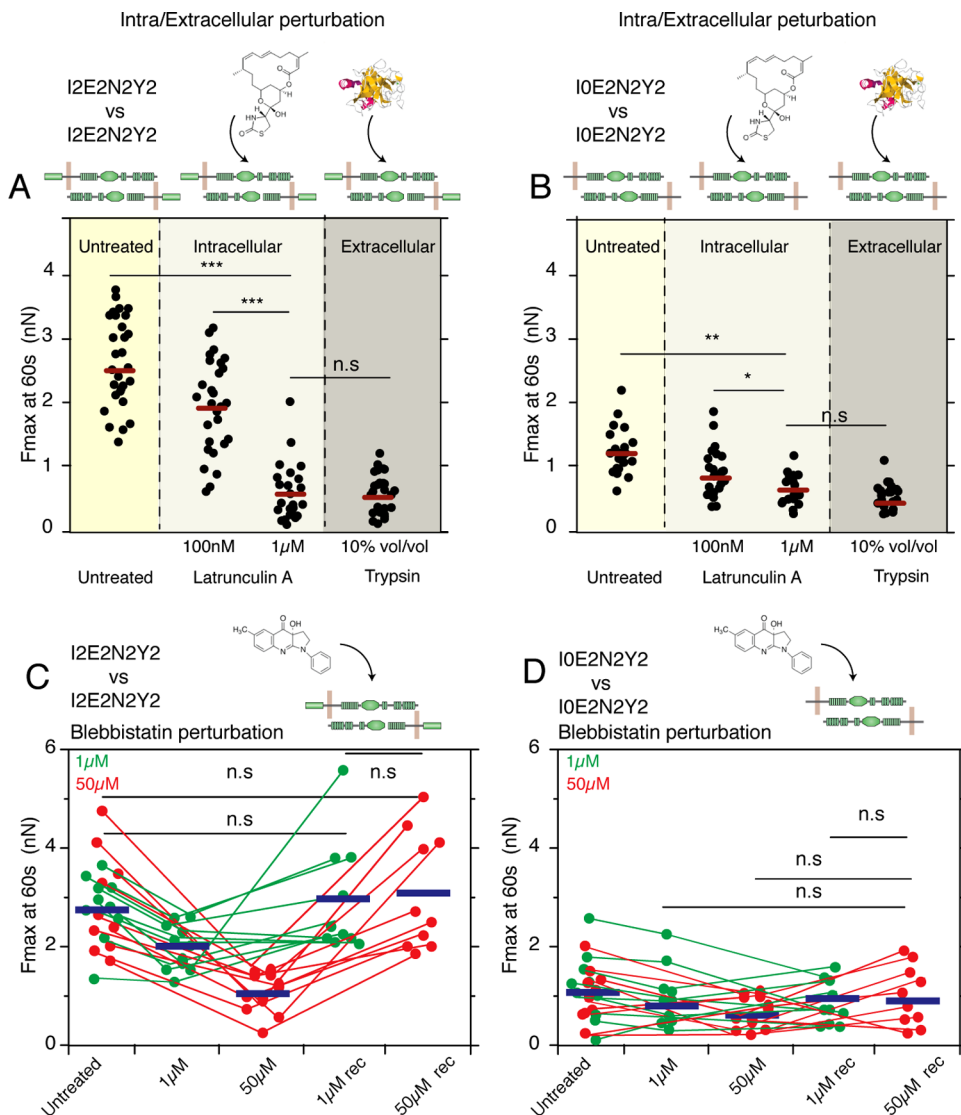


**Figure 3.** Perturbations affecting teneurin mediated cell–cell adhesion. Effect of latrunculin A or trypsin on the homophilic cell–cell adhesion mediated by (A) full-length teneurin-2 (I2E2N2Y2) or (B) teneurin-2 lacking the intracellular domain (I0E2N2Y2). In the presence of sufficient latrunculin A, which perturbs the actomyosin cortex,<sup>15</sup> the teneurin mediated strong homophilic cell–cell adhesion disappears. Control experiments using trypsin to unspecifically cleave cell adhesion molecules from the cell surface show that the low adhesion of cell couples having a perturbed actomyosin cortex resembles the unspecific adhesion between cells in the presence of trypsin. (C,D) Homophilic adhesion force established between cells that overexpress (C) full-length teneurin-2 (I2E2Y2N2) or (D) teneurin-2 lacking the intracellular domain (I0E2Y2N2) in the presence of 1  $\mu$ M (green lines) and 50  $\mu$ M (red lines) blebbistatin and during photoactivation of blebbistatin.<sup>17</sup> Mean cell–cell adhesion forces are shown as blue lines.

**Homophilic Recognition and Adhesion Strengthening Inhibits Nb2a Neurite Outgrowth.** To test whether teneurin-mediated homophilic cell–cell adhesion plays a role in guiding neurite outgrowth, we used Nb2a neuroblastoma cells as model system that differentiates and extends neurites upon serum removal.<sup>18</sup> First we plated Nb2a cells either on a substrate coated with purified recombinant extracellular domains (Supporting Information Figure S1E) of teneurin-2 or with polylysine as control. After transient transfection with either GFP-tagged teneurin-2 or RFP-tagged teneurin-1 we switched the Nb2a cells to serum-free medium. Teneurin-2 transfected Nb2a cells did not grow neurites on a teneurin-2 coated substrate, in contrast to the neighboring untransfected cells, while neurite outgrowth of teneurin-2 overexpressing cells remained unaffected on the control substrate (Figure 4A). In contrast, teneurin-1 overexpressing cells grew neurites on

teneurin-2 extracellular domain as well as polylysine-coated substrates (Figure 4A). Therefore we conclude that the altered growth behavior of teneurin-2 overexpressing cells originated from interactions with teneurin-2 extracellular domains coating the substrate (Figure 4A). These results indicate that homophilic interactions between teneurins of neuronal cells inhibit neurite outgrowth. To quantify this inhibition and to identify the teneurin domains involved, we engineered Nb2a cells stably overexpressing teneurin-2, and teneurin-2 constructs lacking the YD repeats, the entire extracellular domain, or the intracellular domain. The overexpression of teneurin constructs was monitored for every cell line as described for HEK293 cells (Figure 4B and Supporting Information Figure S4A–C). When plated onto substrates coated with extracellular domains from teneurin-2, neurite outgrowth of Nb2a cells overexpressing teneurin-2 was significantly reduced (Figure 4C(i)). In contrast,

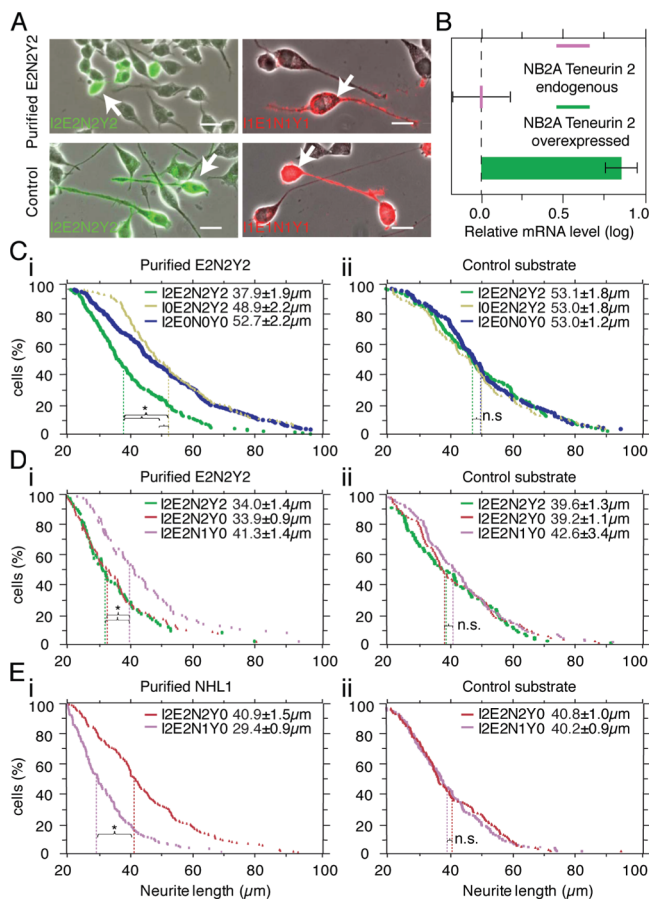


**Figure 4.** NHL domain-mediated teneurin interaction inhibits neurite outgrowth. (A) Nb2a cells transiently transfected with constructs overexpressing either GFP-full-length teneurin-2 (I2E2N2Y2) or RFP-teneurin-1 (I1E1N1Y1) were seeded on coverslips coated with purified extracellular domains from teneurin-2 (E2N2Y2; top panel) or, as control, with polylysine (bottom panel). Neurite outgrowth was induced in serum free media and overlays of phase contrast and fluorescence pictures are shown to discriminate between transfected (green or red, pointed at by arrows) and nontransfected cells only visible by phase contrast. Scale bars, 20  $\mu\text{m}$ . (B) Transcript levels of endogenous and overexpressed teneurin-2 in stably transfected Nb2a cells. (C) Quantification of neurite outgrowth on the extracellular domain of teneurin-2 (E2N2Y2) for Nb2a cells stably overexpressing full-length teneurin-2 (I2E2N2Y2), and teneurin-2 constructs with deleted intracellular (I0E2N2Y2) or deleted extracellular (I2E0NOY0) domains. (D) Quantification of neurite outgrowth on coverslips coated with extracellular domains of teneurin-2 (E2N2Y2) using Nb2a cells overexpressing teneurin-2 constructs with deleted YD repeats (I2E2N2Y0) or with the NHL domain swapped (I2E2N1Y0). (E) Quantification of neurite outgrowth of Nb2a cells on coverslips coated with teneurin-1 NHL domains (NHL1). Nb2a cells stably overexpressed teneurin-2 constructs with deleted YD repeats (I2E2N2Y0) or with the NHL domain swapped (I2E2N1Y0). Each graph (C–E) shows the percentage of cells with neurite lengths greater than the length indicated on the x-axis. A minimum of 150 cells is analyzed per condition. Dashed lines represent the median value, which is given with the SEM for each construct next to the legend. \* Indicates significant differences ( $p < 0.01$ ) between median neurite lengths calculated by One-Way ANOVA on ranks and n.s. indicates no significance difference.

Nb2a cells overexpressing teneurin-2 lacking the intracellular or the extracellular domains showed neurite lengths as observed for control experiments (Figure 4C(i)). However, when seeded

onto polylysine-coated control substrates, all Nb2a cells showed similar neurite outgrowth and lengths (Figure 4C(ii)). To investigate which extracellular domain inhibited neurite outgrowth we measured neurite lengths of Nb2a cells overexpressing teneurin-2 carrying the NHL2 or teneurin-2 carrying the NHL1 domain (Figure 4D(i)). Only Nb2a cells overexpressing teneurin carrying the NHL2 domain showed significantly reduced neurite lengths on teneurin-2 extracellular domain coated substrates, indicating that homophilic NHL domain interactions are required for teneurins to inhibit neurite outgrowth (Figure 4D(i-ii)). This observation could be confirmed by plating teneurin-2 overexpressing Nb2a cells on NHL1 domain coated substrates. Only if the overexpressed teneurin-2 carried the NHL1 domain, neurite outgrowth was reduced (Figure 4E(i-ii)).

To quantify neurite growth rates we performed time-lapse imaging of Nb2a cells plated on striped micropatterned surfaces that have been functionalized with purified extracellular teneurin-2 domains or NHL1 domains (Supporting Information Figure S4E,F). The results confirmed that as soon as teneurins could establish homophilic interactions via their NHL domains the neurite growth rate attenuated. Furthermore, the experiments highlighted that the neurite growth rate reduced only if the overexpressed teneurins carried intracellular domains.

In summary, these results show that neuronal cells that establish teneurin-mediated homophilic interactions via their NHL domains significantly reduce neurite growth rates. Again, the teneurin intracellular domain plays a central role as it anchors teneurins to the actomyosin cytoskeleton and contributes to the strengthening of the homophilic cell–cell adhesion. This highlights that homophilic recognition and cytoskeletal interactions are important for teneurins to guide neuronal outgrowth.

**Discussion.** In the past, AFM-based SCFS has been frequently applied to quantify the contribution of specific cell surface receptors to animal cell adhesion.<sup>11,12</sup> Here we have introduced the combination of SCFS with cell biological and genetic recombination approaches to quantify the mechanisms of how teneurins establish homophilic interactions and strengthen cell–cell adhesion. Using a variety of teneurin constructs with deleted and swapped teneurin-1 and teneurin-2 domains, SCFS detected that teneurins recognize their homophilic cell adhesion partner by the NHL domain. However, to strengthen NHL domain-mediated cell–cell adhesion, the intracellular teneurin domain is essential (Figure 5). The intracellular teneurin-1 domain has previously been shown to interact with the vinculin-binding protein CAP/ponsin providing a possible link to the actomyosin cytoskeleton.<sup>14</sup> Furthermore, we have found previously that overexpression of teneurin-2 constructs in Nb2a cells required the intracellular domain for the induction of filopodia, the transport of teneurin-2 into neurites and the colocalization of teneurin-2 with the cortical actin cytoskeleton.<sup>10</sup> Indeed our perturbation experiments showed that the intracellular domains anchor teneurin-1 and teneurin-2 to the actomyosin cortex and disruption of the actin cytoskeleton compromised adhesion strengthening (Figure 3). Since longer contact times between cells led to significantly increasing adhesion strengths we envisage that this strengthening may be facilitated by the rearrangement or clustering of teneurins anchored to the cytoskeleton. Such anchorage is also a prerequisite for adhesion strengthening of other cell adhesion receptors and their

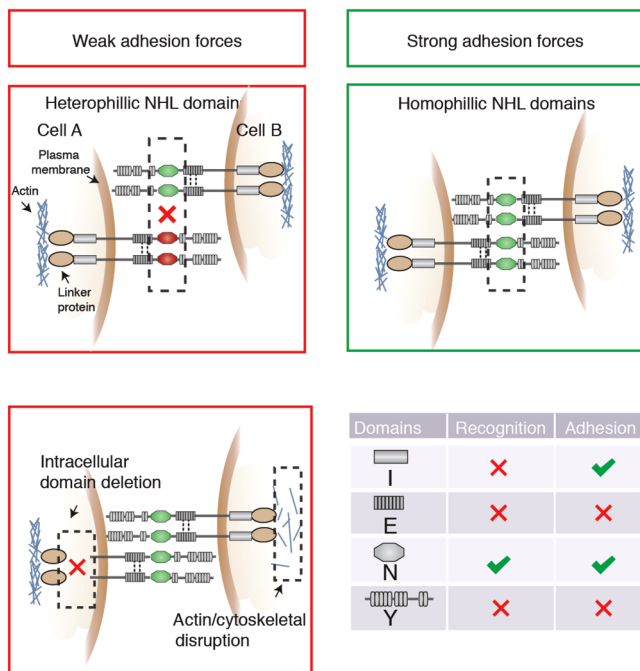


**Figure 5.** Model of teneurin domains selecting and strengthening homophilic cell–cell adhesion. Interaction between the NHL domains controls homophilic recognition between teneurins. Strengthening of homophilic cell adhesion requires the presence of the intracellular domains, which are supposed to connect teneurins to the actin cytoskeleton.

clustering at the interaction sites such as cadherins, SynCAM1, and neitin.<sup>19–21</sup>

Homophilic interactions of teneurin are mediated by C-terminal domains following the EGF-like repeats.<sup>22</sup> These C-terminal domains include the NHL repeats of the NHL domain.<sup>2</sup> NHL repeats are known to form beta-propellers.<sup>23</sup> Thus, it may be speculated that in teneurins the NHL repeats form a beta-propeller domain. We were able to pinpoint the NHL domain to mediate the homophilic interaction between cells overexpressing teneurins. Interestingly, the interaction between other cell surface receptors such as semaphorins and plexins is also mediated by propeller–propeller interactions.<sup>24,25</sup> However, whereas in the case of semaphorins and plexins the beta-propellers promote heterophilic pairing, we observed that the NHL propeller domains from teneurins establish homophilic recognition between cells.

The teneurin-mediated homophilic recognition and formation of cell adhesion partners has functional consequences for neurons as it leads to inhibition of neurite outgrowth. The in vitro inhibition of neurite outgrowth is governed by NHL domain interactions and requires the presence of the intracellular domain. Whereas the NHL domain facilitates homophilic recognition, the strengthening of cell adhesion requires in addition the intracellular domains. In absence of the intracellular domain, teneurin cannot stop neurite outgrowth. Because adhesion strengthening of cell adhesion receptors requires clustering at the interaction sites,<sup>19–21,26</sup> we envisage that clustering of teneurins on a growth cone adhering to a substratum exposing the same type of teneurin leads to strong homophilic adhesion. This formation of strong adhesion by teneurins must trigger an intracellular response leading to growth cone arrest. It is reminiscent of the wiring and target finding that depends on the *Drosophila* teneurins ten-m and

ten-a *in vivo*.<sup>3</sup> Projecting olfactory receptor neurons expressing high levels of either teneurin type make connections only with projecting neurons expressing high levels of the same teneurin. These projections can be manipulated by ectopic overexpression of the other type of teneurin.<sup>3</sup> A similar teneurin-mediated mechanism for target finding is expected to contribute to vertebrate neuronal circuit formation, since expression of the same type of teneurins have been observed in interconnected nuclei of the visual system in chicken.<sup>10</sup> Furthermore, teneurin-3 deficient mice or humans suffer from visual deficits representing strong evidence for a crucial role of teneurins in target selection also in vertebrates.<sup>5,6</sup>

The unique combination of our nanotechnological and cell biological and genetic engineering approaches open new opportunities to characterize interaction mechanisms of any given cell adhesion receptor in live cells. Our quantitative SCFS assay unraveled the contribution of individual teneurin domains to cell–cell recognition and to the formation and strengthening of cell–cell adhesion. The mechanistic insights show teneurin domains contributing to target selection through differential cell–cell adhesion. Certainly, an important next step will be to characterize which intracellular mechanisms are activated by teneurins upon target binding and adhesion strengthening. In the near future our combinatorial approach may also include chemical or genetic perturbation methods to characterize how neuronal or other cell surface receptors regulate cell adhesion.

**Materials and Methods.** *Cloning of Teneurin Constructs and Establishment of Cell Strains.* Full-length chicken teneurin-1 (I1E1N1Y1; NM\_204862) fused to an N-terminal RFP-tag and full-length chicken teneurin-2 (I2E2N2Y2; NM\_204097) fused to an N-terminal GFP-tag were cloned into a pcDNA3.1 vector. Subsequent swap and deletion constructs were cloned into the same vector. Swap constructs were generated by overlapping PCR using a 14bp overhang. Swap and deletion constructs (Figure 1A) were cloned using the following domain boundaries (in base pairs). Teneurin-1: Intracellular domain 1–852, EGF domain 853–2310, NHL domain 2311–4428, and YD domain 4429–8118. Teneurin-2: Intracellular domain 1–388, EGF domain 389–2613, NHL domain 2614–4719, and YD domain 4720–8409. All constructs were sequence verified. HEK293 cells (HEK EcR-293; Invitrogen) and Nb2a neuroblastoma cells (ATCC CCL131) were maintained in DMEM media with 10% (vol) fetal calf serum (FCS), 100 mg/mL penicillin and 100 mg/mL streptomycin. Stable cell lines were established by G418 selection and FACS sorted for homogeneous GFP- or RFP-fusion protein expression with the same gating (Supporting Information Figure S1). Cell surface staining of all overexpressed constructs was confirmed by staining the non-permeabilized cells with a polyclonal antibody against the EGF domains of teneurin-1 (anti-EGF) or teneurin-2.<sup>27,28</sup> Z-stacks were acquired on a spinning disk system (Zeiss AxioImager M1 with a Yokogawa CSU-22 scanhead) with 100× magnification. Images were deconvolved using the Huygens remote manager.<sup>29</sup>

To compare the level of overexpression of our teneurin constructs with the expression level of endogenous teneurin, we assessed the transcript levels by real-time Q-PCR. For this, total RNA was isolated from HEK293 or Nb2a cells stably overexpressing teneurin constructs and of nontransfected cells using QiaShredder and the RNA Easy kit (Qiagen) following the manufacturer's protocol. From this RNA preparation, cDNA was generated using the high capacity cDNA reverse

transcription kit (Applied Biosystems) and random hexamer primers. Real-time Q-PCR was performed on these samples with primer pairs specifically designed to recognize teneurin-1 (fw ACCATG CCTAGC ATGGT GCG; rev CCTGTTGCCTGTATCTGAT) and teneurin-2 (fw TGTGCTAAAGCTGCCCTGCC; rev AAGCAATTCAACTCCTCACAGT) of chicken, mouse, and human origin. Data are normalized to mouse GAPDH (fw TTGTGCAGTGCCAGCCTC; rev GCCGTGAGTGGAGTCATACTG) for Nb2a cells or human TBP (fw TGCACAGGAGCCAAGAGTGAA; rev CACATCACAGCTCCCCACCA) for HEK293 cells using SYBR QPCR Supermix with ROX (Invitrogen) on an AbiPrism StepOne Plus system (Applied Biosystems).

**Purification of Recombinant Teneurin Proteins.** The DNA sequence spanning base pairs 1786–8409 encoding the complete extracellular domain of chicken teneurin-2 (E2N2Y2) and the NHL domain spanning base pairs 3330–4530 of teneurin-1 (NHL1) were cloned into a modified pSecTag vector (Invitrogen) containing N-terminal His- and FLAG-tags and a 3C protease site and made compatible with the pOPIN suite (Oxford Protein Production Facility) using InFusion cloning (Clontech) and pOPIN compatible primers.<sup>30</sup> HEK293 cells were selected using Zeocin (Invitrogen) to express the teneurin constructs stably. Secreted constructs were purified from serum-free conditioned media using Probond resin (Invitrogen) following the manual of the supplier. Protein purity was verified SDS Page analysis as shown in Supporting Information Figure S1E,F and mass spectrometry revealed that over 95% of all peptides detected were derived from teneurin-1 and -2, respectively.

**Cell–Cell Adhesion Measurements.** Cell–cell adhesion measurements were conducted with an AFM (Nanowizard II, JPK Instruments) mounted on an inverted fluorescence microscope (Zeiss Axiovert 200, equipped with 20× objective). The setup was extended with a JPK CellHesion module to increase the cell–cell separation distance to 100 μm and used in closed height feedback mode,<sup>31</sup> phase-contrast and fluorescence imaging were used to monitor cellular morphology during adhesion measurements. Each tipless AFM cantilever (NPO-010, Bruker) was calibrated three times using the thermal noise to eliminate errors. Spring constants were within 10% of the nominal value (~60 mN/m). Plasma-activated cantilevers were incubated with 2.5 mg/mL concanavalin A (ConA, Sigma) overnight at 4 °C and carefully rinsed in phosphate buffered saline (PBS) before use. Petri dishes (WPI Inc.) were plasma treated and coated with 1 mg/mL ConA overnight. HEK293 cells were washed with PBS, detached using 1% (vol) ethylenediaminetetraacetic acid (EDTA, Sigma), and plated in Leibowitz medium containing 1% (vol) serum (SCFS measurement medium) onto the ConA substrate and incubated overnight at 37 °C.

For SCFS, cell morphology was characterized by phase-contrast microscopy and teneurin expression controlled by fluorescence microscopy (Supporting Information Figure S1). The ConA-coated cantilever was gently pressed onto a HEK293 cell applying a force of ≈1 nN for ≈3 s. After this, the cantilever was lifted for 2–10 min to allow the cell to attach firmly to the cantilever. This ‘probe-cell’ was then moved above a ‘target-cell’ that was firmly attached to the ConA-coated substrate. Cell adhesion experiments between probe-cell and target-cell (Figure 1D) were performed applying a contact force of 1 nN, contact times ranging from 5–120 s, and 5 μm/s

approach and retract velocities. The contact time was varied randomly for a given cell–cell couple to prevent systematic bias or history effect. Each force–distance (F–D) curve characterizing the adhesion between probe-cell and target-cell was repeated depending on the contact time: 5 s contact time, 5 repetitions; 20 s contact time, 3 repetitions; 60 s, 1 to 2 repetitions, and 120 s being measured once. A resting time of 30 s was given between recording each F–D curve. Each probe-cell was used to test several target-cells. Not more than five F–D curves were taken with any given probe-cell. Cells were observed continuously during the SCFS experiment to judge whether they were intact and stably associated with the cantilever/substrate. F–D curves were analyzed using IgorPro custom-made routines to extract maximum adhesion force (Figure 1D) and cell deformation (Figure 1H) during cell–cell contact. F–D curves were pooled and statistically processed as described (see Statistical Analysis). To perturb actomyosin, cells were preincubated in 1 μM or 100 nM latrunculin A or blebbistatin (Sigma). Because of the mechanical fragility of the chemically perturbed cells no more than one F–D curve was taken per cell. In cases where perturbants and proteins were added during a measurement, a microsyringe (Hamilton) injected the agents into the AFM Petridish heater and the fluid covering the Petri dish was exchanged several times with a WPI Aladdin push–pull pump setup as described.<sup>32</sup>

**Statistical Analysis.** Maximal adhesion force (Fmax) of F–D curves were averaged from experimental repetitions to determine the mean adhesion force of a given cell couple and contact time. These Fmax values were pooled to obtain their distribution. Median, mean, and standard deviation were extracted with Graph prism (GraphpadSoftware) for unpaired Wilcoxon based Mann–Whitney U-tests for significance with a *p* cutoff value of 0.01. *p* values were calculated using Graph prism. Nonparametric tests were applied to SCFS data, because we assumed that the data are not normally distributed. Although no systematic history effect was seen on successive F–D curves taken with one cell, we could not assume that each F–D curve is strictly independent of each other. Furthermore, cell adhesion forces are likely to be dependent on different properties (e.g., more than one type of adhesion molecule), which does not allow us to use parametric tests. Wilcoxon based Mann–Whitney U-tests are distribution independent and can therefore be applied on composite data sets. Pearson’s rank correlation coefficient *R* was computed using Graph prism.

**Neurite Outgrowth Assays.** Sterile 10 mm coverslips were coated with 30 μg/mL purified extracellular teneurin-2 (E2N2Y2) domains, NHL1 domains, or 100 μg/mL poly D-lysine for at least one hour at room temperature (RT) and washed twice with PBS. Coverslips were placed in 4-well tissue culture dishes (Greiner bio-one) and 2 × 10<sup>4</sup> cells per dish were seeded in 10% FCS in DMEM. The next day the medium was changed to serum-free DMEM to induce Nb2a differentiation.<sup>18</sup> After 24 h cells were fixed with 4% paraformaldehyde for 7 min at RT and stained with rhodamine-coupled phalloidin (Cytoskeleton Inc.) for 30 min at RT and mounted on glass slides. Fluorescence microscopy (Olympus IX70) images were taken at 10× magnification and neurite lengths were manually traced using the NeuronJ plug-in for ImageJ.<sup>33</sup> Only neurites longer than the cell diameter were considered. At least 150 neurites per condition were measured and statistical significance was tested using the One-Way ANOVA on ranks using the GraphPad InStat software.

## ■ ASSOCIATED CONTENT

### ● Supporting Information

FACS sorting and cell surface staining for homogeneous teneurin expression (Figure S1), cell adhesion forces measured for different teneurin constructs having their domains deleted (Figure S2), cell adhesion forces measured for different teneurin constructs having their domains swapped (Figure S3), and data showing the teneurin purification, teneurin substrate coating efficiency, and fluorescence imaging of the neurite outgrowth (Figure S4). This material is available free of charge via the Internet at <http://pubs.acs.org>.

## ■ AUTHOR INFORMATION

### Corresponding Author

\*E-mail: (D.J.M.) daniel.mueller@bsse.ethz.ch; (R.C.-E.) ruth.chiquet@fmi.ch.

### Author Contributions

<sup>†</sup>J.B. and R.S. contributed equally.

R.S. performed all SCFS experiments and determined cortex tension. J.B. made all constructs, developed all cell strains, and recorded fluorescence images. R.S. and J.B. performed neurite outgrowth assays. All authors designed the experiments and wrote the paper.

### Notes

The authors declare no competing financial interests.

## ■ ACKNOWLEDGMENTS

We thank R. Fässler, J. Helenius, P. Scheiffele, M. Stewart, and R. Tucker for critical reading of the manuscript. This work was supported by the European Union (FP7/2007–2013 Grant 211800) and the Swiss National Science Foundation (SNF). We thank H. Kohler for technical help with FACS sorting of cells and L. Gelman and S. Bourke for help with microscopy and live cell imaging.

## ■ ABBREVIATIONS

AFM, atomic force microscopy; EGF domain, epidermal growth factor domain; GFP, green fluorescent protein; h, hour; HEK293 cells, human embryonic kidney 293 cells; FACS, fluorescence activated cell sorting; Nb2a cells, neuroblastoma Nb2a cells; NHL domain, NCL-1, HT2A and Lin-41 domain; NHL1 domain, NHL domain from teneurin-1; NHL2 domain, NHL domain from teneurin-2; nN,  $10^{-9}$  (nano) Newton; RFP, red fluorescent protein; s, second; SCFS, single-cell force spectroscopy; YD, tyrosine aspartate domain

## ■ REFERENCES

- (1) Sanes, J. R.; Yamagata, M. Many paths to synaptic specificity. *Annu. Rev. Cell. Dev. Biol.* **2009**, *25*, 161–195.
- (2) Tucker, R. P.; Beckmann, J.; Leachman, N. T.; Scholer, J.; Chiquet-Ehrismann, R. Phylogenetic analysis of the teneurins: conserved features and premetazoan ancestry. *Mol. Biol. Evol.* **2012**, *29*, 1019–1029.
- (3) Hong, W.; Mosca, T. J.; Luo, L. Teneurins instruct synaptic partner matching in an olfactory map. *Nature* **2012**, *484*, 201–207.
- (4) Mosca, T. J.; Hong, W.; Dani, V. S.; Favoloro, V.; Luo, L. Trans-synaptic teneurin signalling in neuromuscular synapse organization and target choice. *Nature* **2012**, *484*, 237–241.
- (5) Leamey, C. A.; Merlin, S.; Lattof, P.; Sawatari, A.; Zhou, X.; Demel, N.; Glendining, K. A.; Oohashi, T.; Sur, M.; Fassler, R. Ten\_m3 regulates eye-specific patterning in the mammalian visual pathway and is required for binocular vision. *PLoS Biol.* **2007**, *5*, e241.
- (6) Aldahmesh, M. A.; Mohammed, J. Y.; Al-Hazzaa, S.; Alkuraya, F. S. Homozygous null mutation in ODZ3 causes microphthalmia in humans. *Genet. Med.* **2012**, *14*, 900–904.
- (7) Kenzelmann, D.; Chiquet-Ehrismann, R.; Tucker, R. P. Teneurins, a transmembrane protein family involved in cell communication during neuronal development. *Cell. Mol. Life Sci.* **2007**, *64*, 1452–1456.
- (8) Young, T. R.; Leamey, C. A. Teneurins: important regulators of neural circuitry. *J. Biochem. Cell Biol.* **2009**, *41*, 990–993.
- (9) Oohashi, T.; Zhou, X. H.; Feng, K.; Richter, B.; Morgelin, M.; Perez, M. T.; Su, W. D.; Chiquet-Ehrismann, R.; Rauch, U.; Fassler, R. Mouse ten-m/Odz is a new family of dimeric type II transmembrane proteins expressed in many tissues. *J. Cell Biol.* **1999**, *145*, 563–577.
- (10) Rubin, B. P.; Tucker, R. P.; Brown-Luedi, M.; Martin, D.; Chiquet-Ehrismann, R. Teneurin 2 is expressed by the neurons of the thalamofugal visual system *in situ* and promotes homophilic cell-cell adhesion *in vitro*. *Development* **2002**, *129*, 4697–4705.
- (11) Benoit, M.; Gabriel, D.; Gerisch, G.; Gaub, H. E. Discrete interactions in cell adhesion measured by single-molecule force spectroscopy. *Nat. Cell Biol.* **2000**, *2*, 313–317.
- (12) Muller, D. J.; Helenius, J.; Alsteens, D.; Dufrene, Y. F. Force probing surfaces of living cells to molecular resolution. *Nat. Chem. Biol.* **2009**, *5*, 383–390.
- (13) Krieg, M.; Arboleda-Estudillo, Y.; Puech, P. H.; Kafer, J.; Graner, F.; Muller, D. J.; Heisenberg, C. P. Tensile forces govern germ-layer organization in zebrafish. *Nat. Cell Biol.* **2008**, *10*, 429–436.
- (14) Nunes, S. M.; Ferralli, J.; Choi, K.; Brown-Luedi, M.; Minet, A. D.; Chiquet-Ehrismann, R. The intracellular domain of teneurin-1 interacts with MBD1 and CAP/ponsin resulting in subcellular codistribution and translocation to the nuclear matrix. *Exp. Cell Res.* **2005**, *305*, 122–132.
- (15) Spector, I.; Shochet, N. R.; Kashman, Y.; Groweiss, A. Latrunculins: novel marine toxins that disrupt microfilament organization in cultured cells. *Science* **1983**, *219*, 493–495.
- (16) Straight, A. F.; Cheung, A.; Limouze, J.; Chen, I.; Westwood, N. J.; Sellers, J. R.; Mitchison, T. J. Dissecting temporal and spatial control of cytokinesis with a myosin II Inhibitor. *Science* **2003**, *299*, 1743–1747.
- (17) Kolega, J. Phototoxicity and photoactivation of blebbistatin in UV and visible light. *Biochem. Biophys. Res. Commun.* **2004**, *320*, 1020–1025.
- (18) Evangelopoulos, M. E.; Weis, J.; Kruttgren, A. Signalling pathways leading to neuroblastoma differentiation after serum withdrawal: HDL blocks neuroblastoma differentiation by inhibition of EGFR. *Oncogene* **2005**, *24*, 3309–3318.
- (19) Pokutta, S.; Weis, W. I. Structure and mechanism of cadherins and catenins in cell-cell contacts. *Annu. Rev. Cell Dev. Biol.* **2007**, *237*–261.
- (20) Fogel, A. I.; Stagi, M.; Perez de Arce, K.; Biederer, T. Lateral assembly of the immunoglobulin protein SynCAM 1 controls its adhesive function and instructs synapse formation. *EMBO J.* **2011**, *30*, 4728–4738.
- (21) Kurita, S.; Ogita, H.; Takai, Y. Cooperative role of nectin-nectin and nectin-afadin interactions in formation of nectin-based cell-cell adhesion. *J. Biol. Chem.* **2011**, *286*, 36297–36303.
- (22) Feng, K.; Zhou, X. H.; Oohashi, T.; Morgelin, M.; Lustig, A.; Hirakawa, S.; Ninomiya, Y.; Engel, J.; Rauch, U.; Fassler, R. All four members of the Ten-m/Odz family of transmembrane proteins form dimers. *J. Biol. Chem.* **2002**, *277*, 26128–26135.
- (23) Edwards, T. A.; Wilkinson, B. D.; Wharton, R. P.; Aggarwal, A. K. Model of the brain tumor-Pumilio translation repressor complex. *Genes Dev.* **2003**, *17*, 2508–2513.
- (24) Liu, H.; Juo, Z. S.; Shim, A. H.; Focia, P. J.; Chen, X.; Garcia, K. C.; He, X. Structural basis of semaphorin-plexin recognition and viral mimicry from Sema7A and A39R complexes with PlexinC1. *Cell* **2010**, *142*, 749–761.
- (25) Janssen, B. J.; Robinson, R. A.; Perez-Branguli, F.; Bell, C. H.; Mitchell, K. J.; Siebold, C.; Jones, E. Y. Structural basis of semaphorin-plexin signalling. *Nature* **2010**, *467*, 1118–1122.

- (26) Chu, Y. S.; Thomas, W. A.; Eder, O.; Pincet, F.; Perez, E.; Thiery, J. P.; Dufour, S. Force measurements in E-cadherin-mediated cell doublets reveal rapid adhesion strengthened by actin cytoskeleton remodeling through Rac and Cdc42. *J. Cell Biol.* **2004**, *167*, 1183–1194.
- (27) Kenzelmann, D.; Chiquet-Ehrismann, R.; Leachman, N. T.; Tucker, R. P. Teneurin-1 is expressed in interconnected regions of the developing brain and is processed in vivo. *BMC Develop. Biol.* **2008**, *8*, 30.
- (28) Rubin, B. P.; Tucker, R. P.; Martin, D.; Chiquet-Ehrismann, R. Teneurins: a novel family of neuronal cell surface proteins in vertebrates, homologous to the drosophila pair-rule gene product Ten-m. *Dev. Biol.* **1999**, *216*, 195–209.
- (29) Ponti, B. P.; Schwarb, P.; Gulati, A.; Bäcker, V. Huygens remote manager: a web interface for high-volume batch deconvolution. *Imaging Microsc.* **2007**, *9*, 57–58.
- (30) Berrow, N. S.; Alderton, D.; Sainsbury, S.; Nettleship, J.; Assenberg, R.; Rahman, N.; Stuart, D. I.; Owens, R. J. A versatile ligation-independent cloning method suitable for high-throughput expression screening applications. *Nucleic Acids Res.* **2007**, *35*, e45.
- (31) Puech, P. H.; Poole, K.; Knebel, D.; Muller, D. J. A new technical approach to quantify cell-cell adhesion forces by AFM. *Ultramicroscopy* **2006**, *106*, 637–644.
- (32) Stewart, M. P.; Toyoda, Y.; Hyman, A. A.; Muller, D. J. Tracking mechanics and volume of globular cells with atomic force microscopy using a constant-height clamp. *Nat. Protoc.* **2012**, *7*, 143–154.
- (33) Meijering, E.; Jacob, M.; Sarria, J. C.; Steiner, P.; Hirlimann, H.; Unser, M. Design and validation of a tool for neurite tracing and analysis in fluorescence microscopy images. *Cytometry A* **2004**, *58*, 167–176.